A&A 465, 541–547 (2007)
DOI: 10.1051/0004-6361:20066360

Astronomy & Astrophysics

An abundance analysis of a chemically peculiar B star – JL 87⋆,⋆⋆

A. Ahmad[1], N. T. Behara[1], C. S. Jeffery[1], T. Sahin[1], and V. M. Woolf[1,2]

[1] Armagh Observatory, College Hill, Armagh BT61 9DG, N. Ireland, UK
e-mail: amir@star.arm.ac.uk
[2] Dept. of Physics, University of Nebraska at Omaha, 6001 Dodge Street, Omaha, Nebraska 68182-0266, USA

Received 7 September 2006 / Accepted 8 January 2007

ABSTRACT

Aims. The aim of this study is to understand the nature and origin of a chemically peculiar star JL 87 by measuring its physical parameters and chemical abundances.
Methods. Physical parameters – effective temperature, surface gravity and helium abundance were measured from a moderate resolution optical spectrum using fully line-blanketed LTE model atmospheres. The effective temperature and extinction were verified by comparing FUSE, IUE spectrophotometry and optical/IR broadband photometry with theoretical flux distributions from LTE model atmospheres. The photospheric chemical abundances were measured from a high-resolution optical spectrum using LTE model atmospheres and spectral synthesis.
Results. On the basis of its physical parameters and chemical abundances, we confirm that JL 87 is a chemically peculiar subluminous B star. It is significantly cooler, has a lower surface gravity and is more helium-rich than previously believed. It is moderately enriched in carbon and nitrogen, but its overall metallicity is slightly subsolar.
Conclusions. The shallow-mixing model of a late core-flash on a white-dwarf cooling track currently provides the most consistent agreement with the observable properties of JL 87.

Key words. stars: chemically peculiar – stars: early-type – subdwarfs – stars: individual: JL 87 – stars: abundances – stars: fundamental parameters

1. Introduction

JL 87 was identified to be a "possibly violet" bright source in a search for faint violet stars at southern galactic latitudes (Jaidee & Lynga 1974). Subsequent spectroscopy showed it to be enriched by a factor 2 in helium, with an unusually strong CII 4267 line (Schulz et al. 1991). As a consequence it was identified with a small group of underluminous helium-rich B stars, including the sdOD stars from the Palomar-Green survey of faint blue stars (Green et al. 1986). Collectively, these became known as helium-rich subdwarf B stars (He-sdB) (Moehler et al. 1990), a primarily spectroscopic classification.

The same object was independently recovered in the Edinburgh-Cape (EC) survey of southern blue stars as EC 21435-7634 with spectral-type "B1:He/sd?" (Kilkenny et al. 1995). An analysis of a $R \sim 1$ Å spectrum allowed Magee et al. (1998) to derive parameters at some variance to those obtained by Schulz et al. (1991), indicating a hot high-gravity star with a very high rotation velocity $v \sin i = 120 \pm 50$ km s^{-1}. Such a result would have indicated a chemically peculiar main-sequence B star, perhaps an intermediate helium star such as CPD −62°2124 (Ardeberg & Maurice 1977).

Whether JL 87 is genuinely a member of this class in view of its modest helium enrichment has been an ongoing question. It has been sufficiently interesting to provoke further study in the ultraviolet (Ahmad & Jeffery 2004) and far-ultraviolet (Lanz et al. 2004).

The initial aim of this project was to measure surface abundances of bright He-sdB stars in order to understand their evolutionary history. Two He-sdB stars with different helium abundances – PG 1544+488 (extremely helium-rich) and JL 87 (moderately helium-rich) – were selected for the study. The He-sdB prototype, PG 1544+488, turned out to be a binary comprising two He-sdB stars (Ahmad et al. 2004) making abundance measurements with existing data very difficult.

In this work we report fundamental atmospheric parameters of JL 87 from a moderate resolution optical spectrum and flux distribution. We also present a fine analysis of the chemical abundances from high-resolution optical spectra. With these new results we aim to identify the nature of this chemically peculiar star. We discuss various disagreements between our results and previous work.

2. Observations

Two high S/N, medium-resolution ($\lambda/\Delta\lambda \approx 10\,000$) blue spectra (3900–5000 Å) of JL 87 were obtained during service observations with the Anglo-Australian Telescope (AAT) and the Royal Greenwich Observatory (RGO) Spectrograph on 2003 May 11. The observations were reduced using standard IRAF routines. Copper-argon arcs were used for the wavelength calibration. The continuum normalization was done by dividing each spectrum with a low-order polynomial fit to a set of continuum points. Great care was taken to ensure that the profiles of the very broad hydrogen Balmer and neutral helium lines were not compromised by this procedure. The two normalized RGO spectra were merged and this was used to measure the principal atmospheric

⋆ Based on observations obtained with the AAT, IUE and FUSE.
⋆⋆ Figure 6 and Table 4 are only available in electronic form at http://www.aanda.org

Table 1. Heliocentric radial velocities for JL 87. Errors are 1σ.

Instrument	HJD − 2 400 000	RV (km s^{-1})
UCLES	50 223.3320	−5.4 ± 3.0
UCLES	51 389.2313	−7.8 ± 3.3
UCLES	52 450.2304	−4.8 ± 1.7
RGO	52 771.2860	−10.8 ± 4.2
RGO	52 771.2999	−2.5 ± 4.1
UCLES	53 609.8788	−6.4 ± 1.4
UCLES	53 609.9002	−6.3 ± 1.3
UCLES	53 609.9217	−6.2 ± 1.3
UCLES	53 611.9822	−5.6 ± 1.4
UCLES	53 612.0036	−5.6 ± 1.3

parameters of effective temperature ($T_{\rm eff}$), surface gravity (g) and helium abundance ($n_{\rm He}$).

A high-resolution ($\lambda/\Delta\lambda \approx 48\,000$) optical blue spectrum (3900–5000 Å) of JL 87 was obtained at the AAT with the University College London Echelle Spectrograph (UCLES) on 1996 May 19. The échelle spectrum was reduced using standard IRAF routines. Thorium-argon arcs were used for the wavelength calibration. Finally, the individual echelle orders were normalized and merged to produce a single spectrum. A detailed description of the data reduction and normalization procedure can be found in Woolf & Jeffery (2002).

Observations of JL 87 were also made with UCLES in 1999, 2002 and 2005. The 2002 UCLES spectrum was also reduced using IRAF routines. The 1999 and 2005 data have been reduced with the ECHOMOP package (Mills et al. 1996). The 1999 spectrum has low signal-to-noise ratio (S/N) due to poor conditions. Hence only the radial velocity was measured from this spectrum.

Finally, we merged the the 1996, 2002 and 2005 spectra into one high S/N spectrum from which chemical abundances were measured. In order to combine the individual observations, we first measured radial velocities from sharp metal lines by cross-correlation with a synthetic spectrum. These are listed in Table 1, corrected to the heliocentric frame. The individual spectra were corrected to the laboratory rest frame and then combined as a weighted mean. Measurements of the inverse variance in the same region of continuum in the individual spectra were used for the weights.

The 1996 spectrum of JL 87 has the highest resolution of all our observations due to the use of a narrow slit. Hence the microturbulent velocity and the projected rotational velocity were measured *only* from the 1996 UCLES spectrum. Chemical abundances were measured from both the 1996 and the merged UCLES spectra.

Chemical abundances are measured using a model atmosphere with an assumed $T_{\rm eff}$, g and $n_{\rm He}$. In early-type stars, these parameters can normally be measured from the strong hydrogen Balmer lines and helium lines in the absorption spectrum. In the case of échelle spectra of JL 87, these broad lines are very sensitive to the adopted normalization. Several lines span more than one échelle order so that it is difficult to remove the blaze function accurately. Therefore the H and He line profiles could not be relied upon in all the UCLES spectra as reduced by us.

In order to recover information from the weak lines in the spectrum, the UCLES spectra were renormalized using the best-fit model to the medium-resolution (RGO) spectrum described above. Having obtained this best-fit spectrum (see Fig. 1), we divide the fit by the UCLES spectrum, smooth the ratio using a Gaussian filter with 120 Å, and then multiply by the original UCLES spectrum. The result is checked by comparing the RGO spectrum with the re-normalized UCLES spectra.

We note that the normalization forms part of an iterative procedure. The best-fit model to the RGO spectrum is a function of the abundances derived from the UCLES spectrum, particularly for C, N and O. We checked that the normalization produced by the adopted best-fit model was consistent with the final abundances reported.

A far-ultraviolet spectrum of JL 87, obtained with the FUSE satellite (PI: Brown) was retrieved from the Multimission Archive at the Space Telescope (MAST). This was combined with the ultraviolet and optical/IR data used by Ahmad & Jeffery (2004) to provide additional wavelength coverage for studying the flux distribution. The FUSE spectrum was binned to the IUE resolution and merged using weights 10:1 in the overlap region (1160–1185 Å).

3. Model atmospheres

The main objective in this investigation was to measure the chemical abundances of JL 87. The method used is an iterative process. We start with an initial grid of model atmospheres with an assumed composition. We then solve for $T_{\rm eff}$, g and $n_{\rm He}$. Using a model atmosphere with these parameters, we solve for the abundances of minor elements. If significantly different from the initial assumed composition, we compute a new set of model atmospheres. The process continues until convergence.

The model atmospheres were computed using the recently improved LTE code STERNE (Behara & Jeffery 2006). The models assume plane-parallel geometry, hydrostatic and radiative equilibrium. The continuous opacity is calculated using photoionization cross-sections from the Opacity Project (OP: 1995, 1997), and the line opacity is treated using an opacity sampling approach. A grid of line-blanketed model atmospheres was calculated with $T_{\rm eff}$ = 17 500 (2500) 32 500 K, log g = 4.00 (0.25) 5.50, and helium abundance by number ($n_{\rm He}$) = 0.10, 0.30 and 0.50. Solar metal abundances were used for the initial grid while the final grid was computed using metal abundances measured from the high-resolution optical spectrum. The initial solar metalicity models were calculated using a microturbulent velocity ($v_{\rm t}$) of 5 km s^{-1}, a value generally used for early type stars (Gies & Lambert 1992). We then measured the microturbulent velocity (see Sect. 4.3) of JL 87 and all subsequent models were computed using $v_{\rm t}$ = 2 km s^{-1}. Synthetic spectra of the models were computed using an updated version of the LTE spectrum synthesis code SPECTRUM (Jeffery et al. 2001), which uses the OP cross-sections for the bound-free opacity calculation.

All the models used in our analysis have been calculated using the LTE approximation. This approximation can be used for JL 87 as it is cooler than 30 000 K, above which NLTE effects become significantly important (e.g. Napiwotzki 1997). In a recent analysis of two hydrogen-rich sdB stars, Przybilla et al. (2006) obtained temperature and gravity shifts of some 1200 K and 0.12 dex respectively by introducing opacity-sampled LTE model atmospheres and a non-LTE line formation code. Given Napiwotzki's result, the bulk of the difference would appear to be due to the improved opacity treatment. Since we also use opacity-sampled LTE model atmospheres, with an improved treatment of the continuous opacities (Behara & Jeffery 2006), systematic errors due to the assumption of LTE are likely to be small.

In measuring abundances, strong lines are known to show stronger departure from LTE than weak lines (e.g.

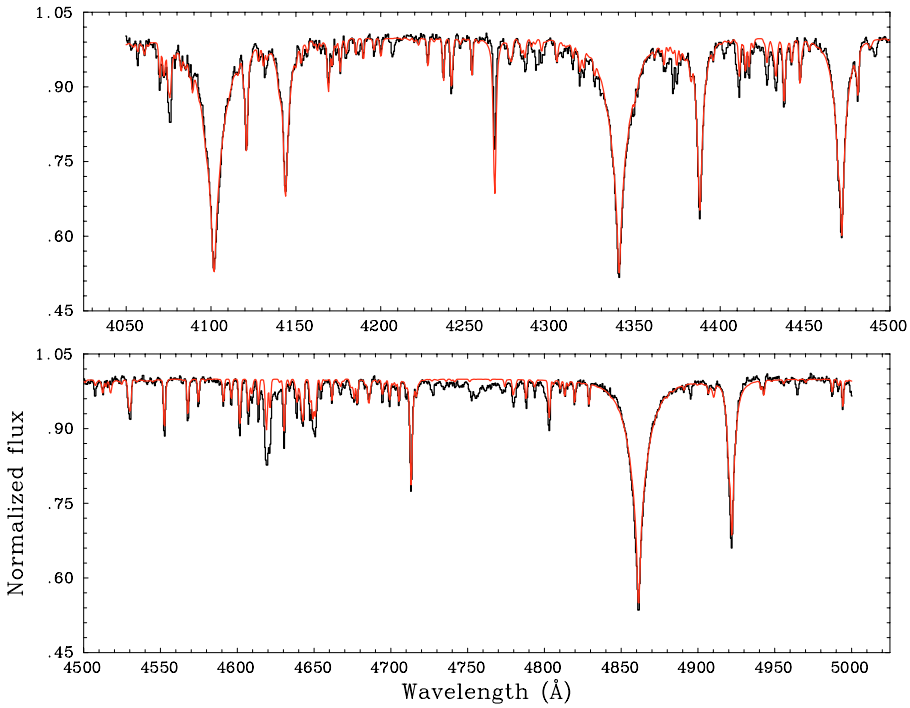

Fig. 1. RGO spectrum of JL 87 (dark) along with best fit (light / red online): $T_{\rm eff} = 25\,800 \pm 1000$, $\log g = 4.8 \pm 0.3$ and $n_{\rm He} = 0.33 \pm 0.02$. This solution was obtained from a model grid with [Fe/H] = −0.3, [C/H] = 0.3, and [N/H] = 0.6 using the solve option in SFIT2.

Table 2. Photospheric chemical abundances of JL 87 given as $\log n$, normalized to $\log \sum \mu n = 12.15$ and compared to the solar values (Grevesse & Sauval 1998).

JL 87	H	He	C	N	O	Ne	Mg	Al	Si	P	S	Ar	Fe
UCLES (merged)	11.62	11.26	8.83	8.77	8.60	8.31	7.36	6.28	7.22	5.30	6.88	6.32	7.51
±	0.07	0.18	0.04	0.23	0.23	0.57	0.33	0.13	0.27	1.69	1.42	0.83	0.32
UCLES (1996)	11.62	11.26	8.80	8.71	8.60	8.20	7.42	6.29	7.17	5.20	6.86	6.27	7.46
±	0.10	0.23	0.06	0.23	0.51	0.72	0.36	0.17	0.32	1.93	1.49	1.68	0.34
Sun	12.00	11.00	8.52	7.92	8.83	8.08	7.58	6.47	7.55	5.45	7.33	6.40	7.50

Przybilla et al. 2006). Our whole spectrum approach to abundance determination means that the influence of individual lines is minimized – in fact we often exclude strong lines from the analysis for just this reason. Any residual errors in the abundances due to the assumption of LTE are likely to be of the same order as the random errors shown in Table 2.

4. Analysis and results

4.1. Physical parameters

The effective temperature, surface gravity and surface helium abundance – $T_{\rm eff}$, g and $n_{\rm He}$ – of JL 87 were measured from the velocity corrected, co-added RGO spectrum in the wavelength range 4050–5000 Å using SFIT2 and a grid of line-blanketed LTE synthetic spectra (cf. Ahmad & Jeffery 2003).

The solve option in SFIT2 (Jeffery et al. 2001) finds the optimal fit in a grid of pre-computed model spectra by χ^2 minimization. Thus $T_{\rm eff}$ is derived simultaneously from the relative strengths of the hydrogen and helium lines and the excitation and ionization equilibria of all elements represented in the spectrum (especially HeI/II, SiII/III/IV), and also simultaneously with $n_{\rm He}$ from the relative strengths of the hydrogen and helium lines *and* g from the profiles of hydrogen and helium lines.

Two regions of spectrum were not used in the fit. The most obvious is that between 4580 and 4640 Å, where a very strong carbon feature dominates the spectrum. The non-LTE physics of this particular feature is not treated in our models; it occurs in both emission and absorption in other hydrogen-deficient stars (Leuenhagen et al. 1994) and is thought to be unusually strong because of autoionization broadening involving several dielectronic CII lines from multiplet 50 (DeMarco et al. 1998). We also excluded the region shortward of 4050 Å, because blending between the broad H and He lines prevented identification of the correct continuum level, even in the RGO spectrum. This part of the spectrum was subsequently renormalized as an independent check of the fit at longer wavelengths.

In practice, this measurement cannot be carried out independently of the chemical composition. Model atmosphere grids have been calculated for a range of metallicity and carbon abundance. A first measurement of $T_{\rm eff}$, g and $n_{\rm He}$ enables an initial model to be chosen from which the overall metallicity and carbon abundance may be measured (see below). If necessary, a new model grid is selected (or computed) and $T_{\rm eff}$, g and $n_{\rm He}$ re-measured. This procedure is repeated to convergence. The final

Table 3. Atmospheric parameters of JL 87. Assumed values are given in parenthesis.

$T_{\rm eff}$ (K)	$\log g$ (cgs)	E_{B-V}	$n_{\rm He}$	Notes
25 800 ± 1000	4.8 ± 0.3	–	0.33 ± 0.02	SFIT2
25 600 ± 800	[4.75]	0.11 ± 0.01	[0.30]	FFIT
29 000 ± 2000	5.5 ± 0.3	–	0.09 – 0.16	L04
28 000	5.2	0.15	0.17	S91

Notes: S91 – Schulz et al. (1991); L04 – Lanz et al. (2004).

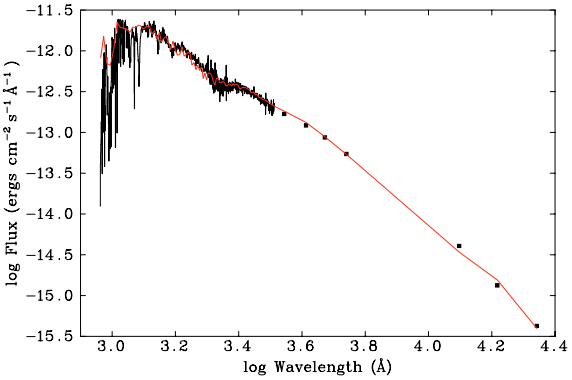

Fig. 2. Flux distribution of JL 87 along with best model fit ($T_{\rm eff}$ = 25 600 ± 800, E_{B-V} = 0.11 ± 0.01 and $\theta = 15.0 \times 10^{-12} \pm 0.2 \times 10^{-12}$).

solution was obtained in a grid with [Fe/H] = −0.3, [C/H] = 0.3, and [N/H] = 0.6. The grid contained models with helium abundances $n_{\rm He}$ = 0.1, 0.3 and 0.5.

The best-fit solution is plotted with the RGO spectrum of JL 87 in Fig. 1. The results are given in Table 3 (labeled SFIT2), where they are compared with results given elsewhere.

4.2. Flux distribution

The flux distribution of JL 87 (1150–22 000 Å) was earlier analysed by Ahmad & Jeffery (2004) using log g and $n_{\rm He}$ values from the literature. With the additional FUSE spectrum (917–1150 Å) and a new set of physical parameters (log g and $n_{\rm He}$) from our spectral analysis, we re-analysed the flux distribution as a consistency check. The model fluxes were computed using a metalicity, [Fe/H] = −0.3 (see Sect. 4.3). The observed fluxes were fitted using the χ^2 minimization program FFIT which solves for the $T_{\rm eff}$, interstellar reddening (E_{B-V}) and angular diameter (θ). The observed flux distribution of JL 87 is plotted with the best-fit model in Fig. 2 and the results are again given in Table 3 (labeled FFIT). The effective temperature of JL 87 obtained from its flux distribution is in good agreement with that measured from the optical spectrum. The new reddening measurement is also in good agreement with that given by Kilkenny et al. (1995), E_{B-V} = 0.09−0.12.

4.3. Chemical abundances

The chemical composition and other parameters were measured from the UCLES spectra. The synth option in SFIT2 assumes a given model atmospheres and computes an emergent spectrum based on an initial composition, microturbulent and rotation velocity – exactly as the LTE code SPECTRUM (Jeffery et al. 2001). Each of these variables may be adjusted, either individually or simultaneously, in order to find the optimum solution by χ^2 minimization. This whole process is iterated with the solution for $T_{\rm eff}$, g and $n_{\rm He}$ described earlier.

The composition of the initial model grid assumed solar abundances for all metals (Grevesse & Sauval 1998). The model atmosphere finally adopted had $T_{\rm eff}$ = 25 000 K, log g = 4.75 and $n_{\rm He}$ = 0.30, with [Fe/H] = −0.3, [C/H] = 0.3, and [N/H] = 0.6. The change in the grid metal abundance produced improvements of $\Delta T_{\rm eff}$ = +500 K, $\Delta \log g$ = +0.06 and $\Delta n_{\rm He}$ = +0.02.

The microturbulent velocity ($v_{\rm t}$) was measured from the 1996 UCLES spectrum – which has the highest resolution – because microturbulence causes intrinsic line broadening comparable to the instrumental broadening. The microturbulence was measured by minimizing the fits to seven OII line profiles to give $v_{\rm t}$ = 2.0 ± 1.0 km s^{-1}. A projected rotational velocity, $v \sin i$ = 0.0 ± 5.0 km s^{-1}, was measured by fitting profiles to the sharp metal lines in the same UCLES spectrum (Fig. 3).

The helium abundance $n_{\rm He}$ was measured from the RGO spectrum in the previous step. Providing there are no other extremely over-abundant ions, this defines $n_{\rm H} \approx 1 - n_{\rm He}$. Abundances of additional elements were measured from both the individual 1996 UCLES spectrum and from the merged UCLES spectrum over the entire wavelength region 3900–5000 Å. Specific wavelength ranges were excluded from the fit in order to avoid regions where atomic data is not well known, or where blending will lead to a badly-conditioned solution. These are shown together with the final solution in Fig. 6 (online only). In practice, χ^2 minimization seems to work best when solving for no more than three elements at a time.

The final photospheric abundances of JL 87 are given in Table 2 for both the merged spectrum and the 1996 spectrum. The errors were estimated by measuring the variance in the elemental abundances taking into account the errors in $T_{\rm eff}$ and g.

The fit to some HeI lines (3964, 4437, 4713 Å) are poor due to difficulties with normalization of the UCLES spectra. However these do not affect the abundance measurements as the hydrogen and helium abundances have been measured from the RGO spectrum and are kept fixed thereafter. Some lines in the spectrum of JL 87 are not included in the linelist used for the spectral analysis because the atomic data is not available. These include some lines of CII, CIII, NII, OII and SiIII. There are also some unidentified lines in the spectrum of JL 87 which are listed in Table 4 (online only). These lines are also seen in other helium-rich stars (e.g. LSE 78: Jeffery 1993). The CII multiplet 1 lines 4735.46, 4737.97, 4744.77, 4747.28 have been excluded as they are not present in the observed spectrum although they are quite strong in the theoretical spectrum. This is also the case with the observed spectrum of carbon-rich LSE 78, where CII multiplet 1 is missing due to CII emission (Heber 1986). Lines from CII multiplets 48 and 49 are too strong in the model compared to the observations. These lines arise from the same lower energy state as multiplet 50 (see Sect. 4.1). The referee has pointed out a possible dependence of quality of the fit on the residual intensity of certain lines. The model underestimates residual intensities of strong SiIII, OII and NII lines but is much better for weak lines. As already discussed above, and nicely demonstrated by Przybilla et al. (2006) strong lines tend to suffer more from non-LTE than do weak lines. Whether this is the correct explanation will require more systematic investigation.

Individual aspects of the surface composition of JL 87 are discussed in turn.

Helium. The helium to hydrogen ratio is, by number $n_{\rm He}/n_{\rm H}$ = 0.49, compared with 0.11 in a solar mix. Such overabundances are not uncommon in chemically peculiar B or He-rich Bp stars, main-sequence stars in which diffusion, stellar wind and magnetic field acts together (e.g. Vauclair 1975; Michaud et al. 1987) to produce unusual local enhancements of surface helium. They are not generally observed in higher-gravity stars such as subdwarf B stars, where radiative levitation forces hydrogen to float on top of the helium (e.g. Heber 1991). It is important to note that an increase in helium number represents a fourfold increase in *mass*. In a solar mix the mass fractions of helium and hydrogen are $\beta_{\rm He} \sim 0.31$ and $\beta_{\rm H} \sim 0.69$ respectively. In JL 87 these

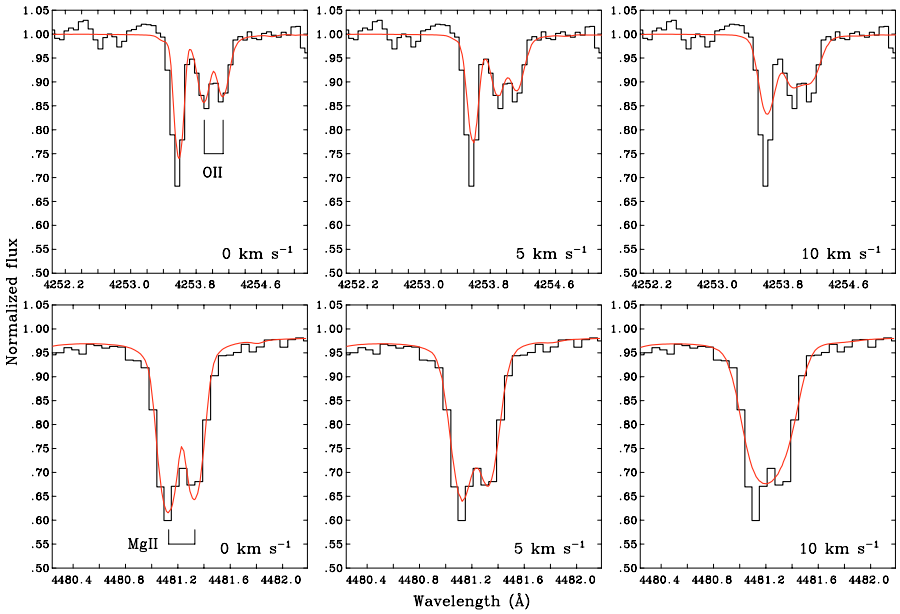

Fig. 3. OII doublet at 4253.90 and 4254.13 Å (*top*) along with the MgII doublet (*bottom*) at 4481.13 and 4481.33 Å in the 1996 UCLES spectrum of JL 87 (dark line) along with synthetic spectrum for various projected rotational velocities, $v \sin i$ = 0.0, 5.0 and 10.0 km s^{-1}.

have become $\beta_{\rm He} \sim 0.62$ and $\beta_{\rm H} \sim 0.36$, thus doubling the helium mass fraction in the atmosphere.

Metallicity. The next feature of the surface composition to note is that JL 87 is somewhat metal poor. Although iron appears to be approximately solar, the measurement depends on relatively few lines of FeIII. Table 4 shows the carbon and iron lines present in the optical spectrum to illustrate the numbers of lines on which these measurements are based. By comparison, magnesium, aluminium, silicon, phosphorus and sulphur are all depleted by ∼0.31 dex, suggesting an overall metallicity [Fe/H] = −0.3.

Nitrogen. In contrast, nitrogen is substantially enhanced. If [Fe/H] = 0.0, the overabundance is 0.85 ± 0.11 dex, or a factor seven (±three). With [Fe/H] = −0.3, the overabundance becomes a factor fourteen (±six). This is almost certainly linked to the high helium abundance *if* the helium is fresh helium – produced by nuclear reactions within the star – rather than being original helium which has been concentrated at the surface. For example, if [Fe/H] = −0.3, then the original abundances for C, N and O should have been 8.22, 7.62 and 8.53 respectively (log by number). Since carbon and oxygen are converted to nitrogen in the hydrogen-burning CNO cycle, the resulting nitrogen abundance in any material which has been either partially or fully processed can be estimated by converting these numbers into mass fractions, adding them together, and then converting them back to a number fraction as nitrogen. In this case, the anticipated abundance of nitrogen would be roughly 8.65 (log by number), an overabundance by a factor ∼11 in line with the observation.

Carbon and oxygen. With a mass fraction of 0.62, roughly half of the surface helium is likely to have come from CNO-processed hydrogen. Therefore there should be some depletion of carbon and oxygen to match, i.e. the abundances should be approximately half the initial abundance, or somewhere between 7.92 and 8.22 for carbon (log by number) and between 8.23 and 8.53 for oxygen, depending on [Fe/H]. With an observed abundance of 8.60 ± 0.25 (log by number) oxygen may be depleted, but less than expected. However carbon is *overabundant* by ∼0.3−0.6 dex, implying that additional carbon from 3α-processed helium is also present. Table 4 lists the strong carbon lines visible in the UCLES spectrum of JL 87.

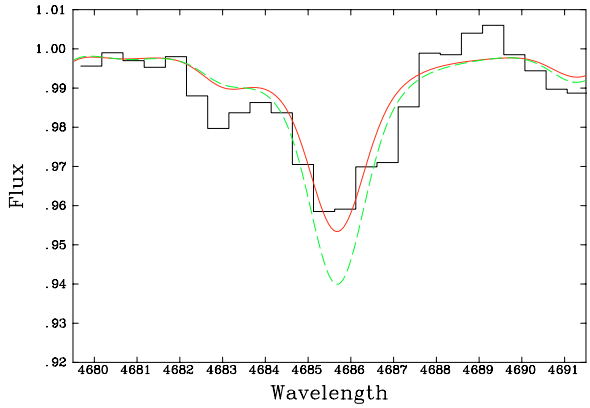

Fig. 4. The observed HeII 4686 line (histogram) of JL 87 plotted with theoretical profiles (smooth lines) computed using [Fe/H] = −0.3 and $v_{\rm t}$ = 2 km s^{-1}. The model on the top (continuous line) is computed with $T_{\rm eff}$ = 25 600 K, log g = 4.75 and $n_{\rm He}$ = 0.30 while the second model (dotted line) is computed with $T_{\rm eff}$ = 28 000 K, log g = 5.00 and $n_{\rm He}$ = 0.10.

4.4. Previous work

There is significant disagreement between our estimates of the physical parameters of JL 87 and previous work. To begin with our estimate of the surface gravity is 0.5–0.8 dex lower than that of Schulz et al. (1991) and Lanz et al. (2004). The latter argued that ignoring carbon in the model atmosphere calculations can lead to an underestimate of log g by 0.5. It appears to us that in testing the importance of carbon, Lanz et al. (2004) compared H+He-only models with models including metals and showed that omitting metals from the model affects the helium line profiles and leads to an underestimate of g. Although they attribute the effect to carbon and nitrogen, the specific contribution of these elements is not distinguished from the contribution of all other metals. All our model atmospheres include all metal lines for which we have data. We found that increasing the carbon in the model to the abundance measured in JL 87 produces *no* significant change in log g (see Sect. 4.3).

Our effective temperature is ∼3000 K lower than previously estimated (see Table 3). The effective temperature of

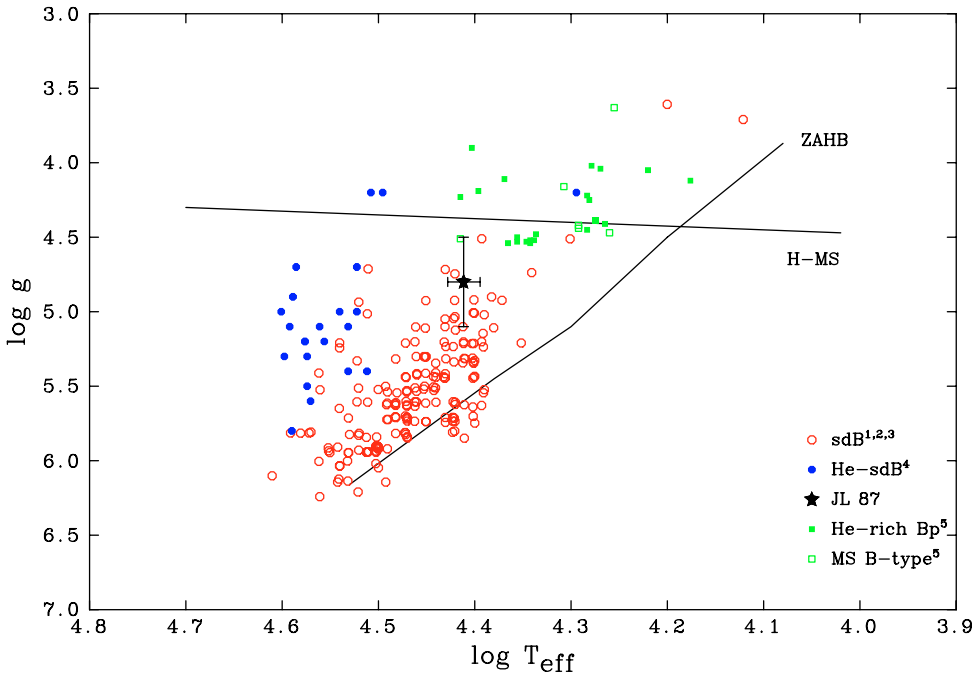

Fig. 5. Position of JL 87 on the log g–$T_{\rm eff}$ diagram along with other B-type stars. The sdB data has been jittered slightly by adding small random numbers $\delta T_{\rm eff}$ and $\delta \log g$ (where $0 < \delta T_{\rm eff} < 200$ and $0 < \delta \log g < 0.05$). The hydrogen main sequence (H-MS) is given for $X = 0.7$ and $Z = 0.02$ from Claret & Gimenez (1992). The zero age extended horizontal branch (ZAHB) is taken from Dorman et al. (1993).
References : [1]Moehler et al. (1990); [2]Saffer et al. (1994); [3]Maxted et al. (2001); [4]Ahmad & Jeffery (2003) and [5]Zboril & North (1999).

~25 800 ± 1000 K for JL 87 is strongly constrained by the temperature sensitive HeII 4686 line (Fig. 4). The optical spectrum may also be fit with a higher temperature and surface gravity, but *only* by excluding HeII 4686.

Our earlier study of the flux distribution of JL 87 found $T_{\rm eff} = 28\,100$ K (Ahmad & Jeffery 2004). In our current analysis we find a lower temperature; this is primarily due to adopting a lower value of $E_{(B-V)} = 0.11$ mag. We had previously noted (Ahmad & Jeffery 2004) that there are a number of local minima in χ^2 corresponding to a number of possible $T_{\rm eff}$ and $E_{(B-V)}$ solutions for each star. In order to remove the degeneracy between these two parameters, we chose the solution with $T_{\rm eff}$ closest to a spectroscopically determined temperature and used the corresponding values for $E_{(B-V)}$. For JL 87 we had chosen $E_{(B-V)} = 0.16$ as it provided $T_{\rm eff}$ close to that measured from the optical spectrum by Schulz et al. (1991). This solution can now be excluded following our spectral analysis (Fig. 4).

The differences between our surface gravity and helium abundance measurements and previous results are almost certainly a consequence of our using a lower effective temperature.

The other disagreement is the projected rotational velocity ($v \sin i$) of JL 87. The metal lines in the optical spectrum are quite sharp and can be reproduced with the projected rotational velocity, $v \sin i \leq 5\,{\rm km\,s^{-1}}$. Such a low $v \sin i$ is typical of most subdwarf B stars (Edelmann et al. 2001). The low $v \sin i$ for JL 87 is illustrated in Fig. 3 where the resolved OII 4254 doublet and MgII 4481 doublet can only be reproduced by $v \sin i \leq 5\,{\rm km\,s^{-1}}$.

Lanz et al. (2004) measured $v \sin i = 30\,{\rm km\,s^{-1}}$ from the sharp metal lines in the FUSE spectrum. Magee et al. (1998) measured $v \sin i = 120 \pm 50$ km s^{-1} from a moderate resolution optical spectrum. This might have been due to the use of broad hydrogen Balmer lines and a model template with too high a $T_{\rm eff}$, since Balmer lines become narrower with increasing $T_{\rm eff}$. There is also no evidence of radial-velocity variability in JL 87 (Table 1) which might otherwise account for the high values of $v \sin i$.

5. What is JL 87?

We have established that JL 87 is a helium-rich early-type B star, with a surface gravity higher than that anticipated for a main-sequence star, but not quite so high as for a typical subdwarf B star (Fig. 5). It is slightly metal-deficient, with nitrogen enriched by CNO processing, and possibly some additional carbon enrichment. There is no evidence that JL 87 is a binary although this cannot be ruled out entirely. There is no evidence of radial velocity variation (Table 1) or of any flux excess in the red or infrared. We have not yet ruled out completely the possibility that the spectrum may vary.

It is known that some main-sequence B stars show strong helium enrichment (e.g. Zboril & North 1999). They have strong magnetic fields, are "slow" rotators ($v \sin i < 100\,{\rm km\,s^{-1}}$) compared to other main-sequence stars, show variable spectra and normal CNO abundances. Unless the inclination angle is close to zero, the very slow rotation and the signature of CNO-processing observed in JL 87 are inconsistent with it being a chemically peculiar main-sequence star. This possibility also seems to be excluded by its galactic position. With $m_V = 12.0$ and $E_{B-V} = 0.11$, a main-sequence B star with $T_{\rm eff} = 25\,000$ K would lie at a distance of ~9.4 kpc, placing JL 87 implausibly some 5.5 kpc above the galactic plane.

Therefore JL 87 must be an evolved low-mass star of some sort. The surface gravity suggests a link with hot subdwarfs including the H-rich sdB stars, or with the He-rich sdO stars. In other words, it is not low enough to be a post-AGB star, but it is too low to be, currently, a blue or extreme horizontal-branch star, as are the true sdB stars. It seems more likely that it is evolving either toward or away from the extreme horizontal-branch, but to say more would be speculative. The so-called He-sdB prototype, PG 1544+488, is a binary containing *two* He-sdB stars which implies that at least some of these stars are produced by close-binary evolution. JL 87 is not a close binary.

It has been proposed (Lanz et al. 2004) that stars evolving with very high mass loss on the red giant branch can undergo a very late helium core flash while on the helium white dwarf cooling track. Convective flash mixing of the envelope then

forms a helium-rich and carbon-rich hot subdwarf. Lanz et al. (2004) argued that their analyses of the FUSE spectra of two He-sdB stars, including JL 87, support this idea. Our new result for the surface gravity of JL 87 is ∼0.4 dex lower than that for the shallow-mixing evolutionary tracks presented by Lanz et al. (2004). Meanwhile our carbon and nitrogen abundances (0.69% carbon and 0.70% nitrogen by mass) are consistent with the predictions of the shallow-mixing model (0.8% carbon and 0.5% nitrogen). Thus this model may be attractive. The only question is how the high mass loss is produced. If it is necessary to produce this by common-envelope ejection or unstable Roche lobe overflow, the absence of a detectable binary companion may represent a problem. This could be mitigated by the presence of an unseen white dwarf companion in a long-period orbit.

Iben & Tutukov (1986) on the other hand have suggested that the merger of two white dwarfs (WD) can produce a hot subdwarf with a depleted hydrogen atmosphere. More recently this has been modelled by Saio & Jeffery (2000) to explain the origin of EHe stars. Some of these EHe stars may evolve into He-sdB stars. The binary merger model can explain both carbon-rich and carbon-poor He-sdB stars. A merger of two helium WDs can produce a carbon-poor He-sdB star. A low-mass CO+He WD merger might produce a star which resembles a carbon-rich He-sdB during its evolution to the WD track. The merger models can explain a range of chemical abundances. However it is not clear how much hydrogen could survive in any such merger since models are only available for extremely helium-rich stars (Saio & Jeffery 2000). Evolutionary models for binary white dwarf mergers that produce moderately helium-rich stars such as JL 87 have not been computed.

6. Conclusions

We have measured physical parameters of JL 87 from a moderate resolution optical spectrum and its IR/optical/UV flux distribution. These confirm that JL 87 is a hot chemically peculiar subluminous B star, although it is substantially cooler than most helium-rich hot subdwarfs.

The surface composition of JL 87 has been measured from a high-resolution optical spectrum with greater precision than before. The mass fractions of hydrogen and helium are 0.36 and 0.62 respectively. The overall metallicity, measured from a variety of light ions excluding C, N and O, is ∼−0.3 dex. Nitrogen is enhanced by an amount (∼1.1 dex) sufficient to justify the idea that the helium enrichment has been produced by a mixture of CNO-processed helium with unprocessed material. Oxygen is underabundant, roughly consistent with its destruction in processed layers by the CNO bi-cycle. Carbon is overabundant by ∼0.6 dex, indicating the presence of 3α processed material.

Repeated radial-velocity measurements indicate no evidence of binarity and, as a result, make it puzzling as to how JL 87 has acquired its peculiar surface composition. "Flash mixing" appears to offer a possible fit to the observed surface properties, but needs a mechanism to explain very high mass-loss on the giant branch. A low-mass white dwarf merger seems less attractive. The detection of a binary companion in a large orbit would greatly assist the resolution of this question, while more substantial theoretical predictions focused specifically on nucleosynthesis products, mass loss and mixing mechanisms would be invaluable.

Acknowledgements. This research is supported by the UK Particle Physics and Astronomy Research Council through grants PPA/G/S/2002/00546 and PPA/G/O/2003/00044 and by the Northern Ireland Department of Culture, Arts and Leisure (DCAL). This research has made use of NASA's ADS. Some of the data presented in this paper were obtained from the Multimission Archive at the Space Telescope Science Institute (MAST). STScI is operated by the Association of Universities for Research in Astronomy, Inc., under NASA contract NAS5-26555. Support for MAST for non-HST data is provided by the NASA Office of Space Science via grant NAG5-7584 and by other grants and contracts. We thank the referee for useful comments and suggestions.

References

Ahmad, A., & Jeffery, C. S. 2003, A&A, 402, 335
Ahmad, A., & Jeffery, C. S. 2004, A&A, 413, 323
Ahmad, A., Jeffery, C. S., & Fullerton, A. W. 2004, A&A, 418, 275
Ardeberg, A., & Maurice, E. 1977, A&AS, 28, 153
Behara N. T., & Jeffery, C. S. 2006, A&A, 451, 643
Claret, A., & Gimenez, A. 1992, A&AS, 96, 255
de Marco, O., Storey, P. J., & Barlow, M. J. 1998, MNRAS, 297, 999
Dorman, B., Rood, R. T., & O'Connell, R. W. 1993, ApJ, 419, 596
Edelmann, H., Heber, U., & Napiwotzki, R. 2001, Astron. Nachr., 322, 401
Gies, D. R., & Lambert, D. L. 1992, ApJ, 387, 673
Green, R. F., Schmidt, M., & Liebert, J. 1986, ApJS, 61, 304
Grevesse, N., & Sauval, A. J. 1998, Space Sci. Rev., 85, 161
Heber, U. 1986, Hydrogen Deficient Stars and Related Objects, ASSL 128, IAU Colloq., 87, 73
Heber, U. 1991, Evolution of Stars: the Photospheric Abundance Connection, IAU Symp., 145, 363
Iben, I. J., & Tutukov, A. V. 1986, ApJ, 311, 742
Jaidee, S., & Lyngå, G. 1974, Arkiv for Astronomi, 5, 345
Jeffery, C. S. 1993, A&A, 279, 188
Jeffery, C. S., Woolf, V. M., & Pollacco, D. L. 2001, A&A, 376, 497
Kilkenny, D., Luvhimbi, E., O'Donoghue D., et al. 1995, MNRAS, 276, 906
Lanz, T., Brown, T. M., Sweigart, A. V., Hubeny, I., & Landsman, W. B. 2004, ApJ, 602, 342
Leuenhagen, U., Heber, U., & Jeffery, C. S. 1994, A&AS, 103, 445
Magee, H. R. M., Dufton, P. L., Keenan, F. P., et al. 1998, A&A, 338, 85
Maxted, P. F. L., Heber, U., Marsh, T. R., & North, R. C. 2001, MNRAS, 326, 1391
Moehler, S., Richtler, T., de Boer, K. S., Dettmar, R. J., & Heber, U. 1990, A&AS, 86, 53
Michaud, G., Dupuis, J., Fontaine, G., & Montmerle, T. 1987, ApJ, 322, 302
Mills, D., Webb, J., & Clayton, W. 1996, Starlink User Note, 152.3
Napiwotzki, R. 1997, A&A, 322, 256
Przybilla, N., Nieva, M. F., & Edelmann, H. 2006, Balt. Astron., 15, 107
Saffer, R. A., Bergeron, P., Koester, D., & Liebert, J. 1994, ApJ, 432, 351
Saio, H., & Jeffery, C. S. 2000, MNRAS, 313, 671
Saio, H., & Jeffery, C. S. 2002, MNRAS, 333, 121
Schulz, H., Heber, U., & Wegner, G. 1991, PASP, 103, 435
The Opacity Project Team 1995, The Opacity Project, Vol. 1 (Bristol: Institute of Physics)
The Opacity Project Team 1997, The Opacity Project, Vol. 2 (Bristol: Institute of Physics)
Woolf, V. M., & Jeffery, C. S. 2002, A&A, 395, 535
Vauclair, S. 1975, A&A, 45, 233
Zboril, M., & North, P. 1999, A&A, 345, 244

Online Material

Table 4. Strong CII, CIII and FeIII lines present in the optical spectrum of JL 87 along with unidentified lines*.

Carbon			Iron	*
II	II	III	III	
3919.0	4368.3	4056.1	4053.3	4016.0
3920.7	4369.9	4067.9	4139.4	4058.3
4017.3	4372.4	4068.9	4140.5	4208.0
4074.9	4372.5	4070.3	4164.8	4211.4
4075.9	4374.3	4121.8	4166.9	4273.1
4076.5	4375.0	4186.9	4304.8	4329.9
4077.6	4376.6	4315.4	4395.8	4756.4
4267.0	4409.2	4325.6	4419.6	4873.0
4267.3	4410.0	4388.0	4431.0	4885.7
4285.7	4411.2	4515.8		4895.2
4289.9	4411.5	4516.8		4917.1
4291.8	4413.3	4647.4		
4295.9	4618.4	4650.3		
4306.3	4619.2	4651.5		
4307.6	4625.6	4652.1		
4313.1	4630.0	4665.9		
4317.3	4637.6			
4318.6	4638.9			
4321.7	4738.0			
4323.1	4744.8			
4325.8	4953.9			
4326.2	4964.7			

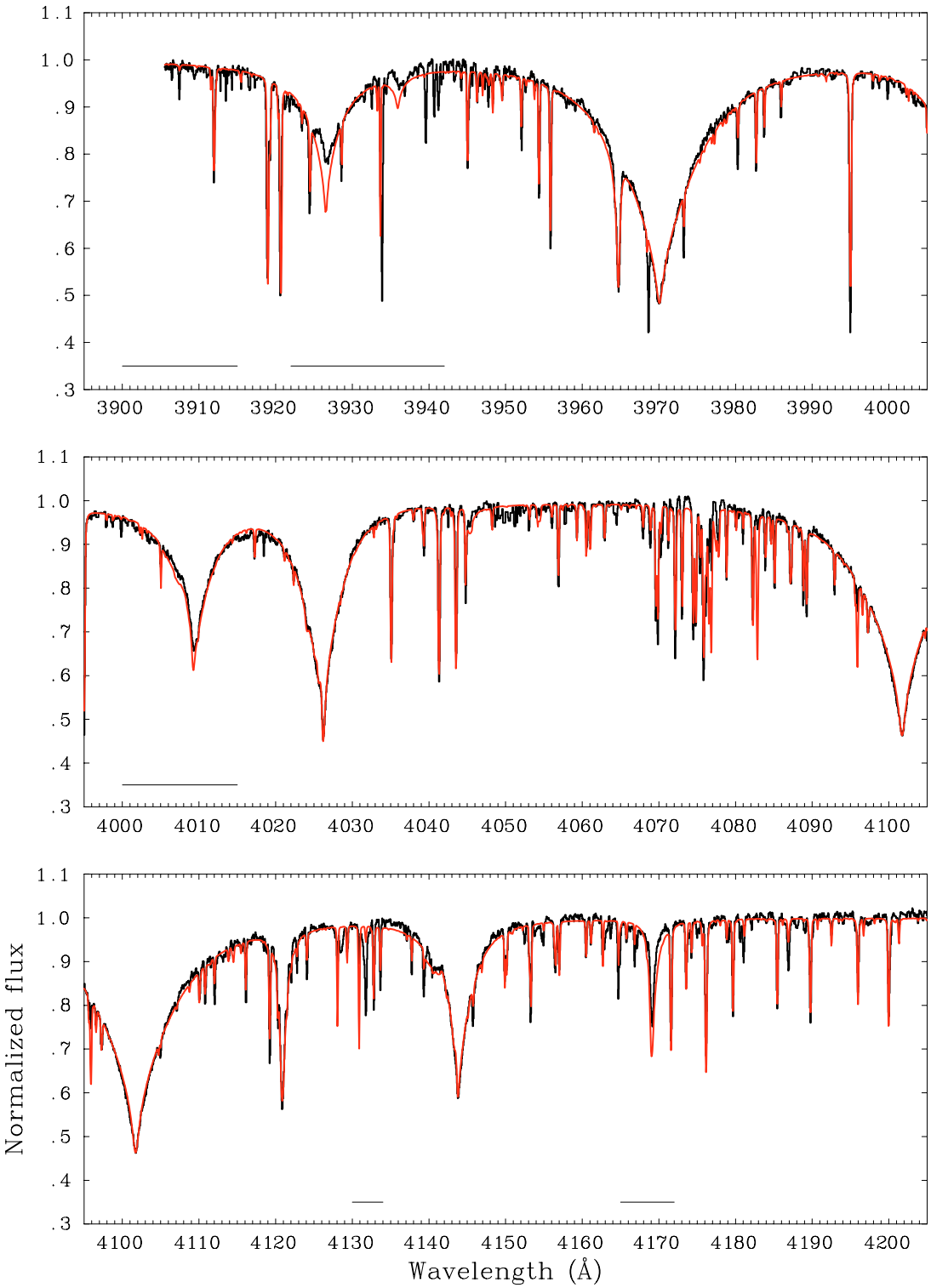

Fig. 6. The merged UCLES spectrum of JL 87 (black) along with best model fit using the synth option in SFIT2 (red). The input model atmosphere had $n_{\rm He} = 0.30$, $T_{\rm eff} = 25\,000$ K, and log $g = 4.75$. The chemical composition of the best-fit solution is shown in Table 3. Other parameters of the fit are $v \sin i = 0$ km s^{-1} and $v_{\rm t} = 2$ km s^{-1}. Horizontal black lines show regions excluded from the χ^2-minimization.

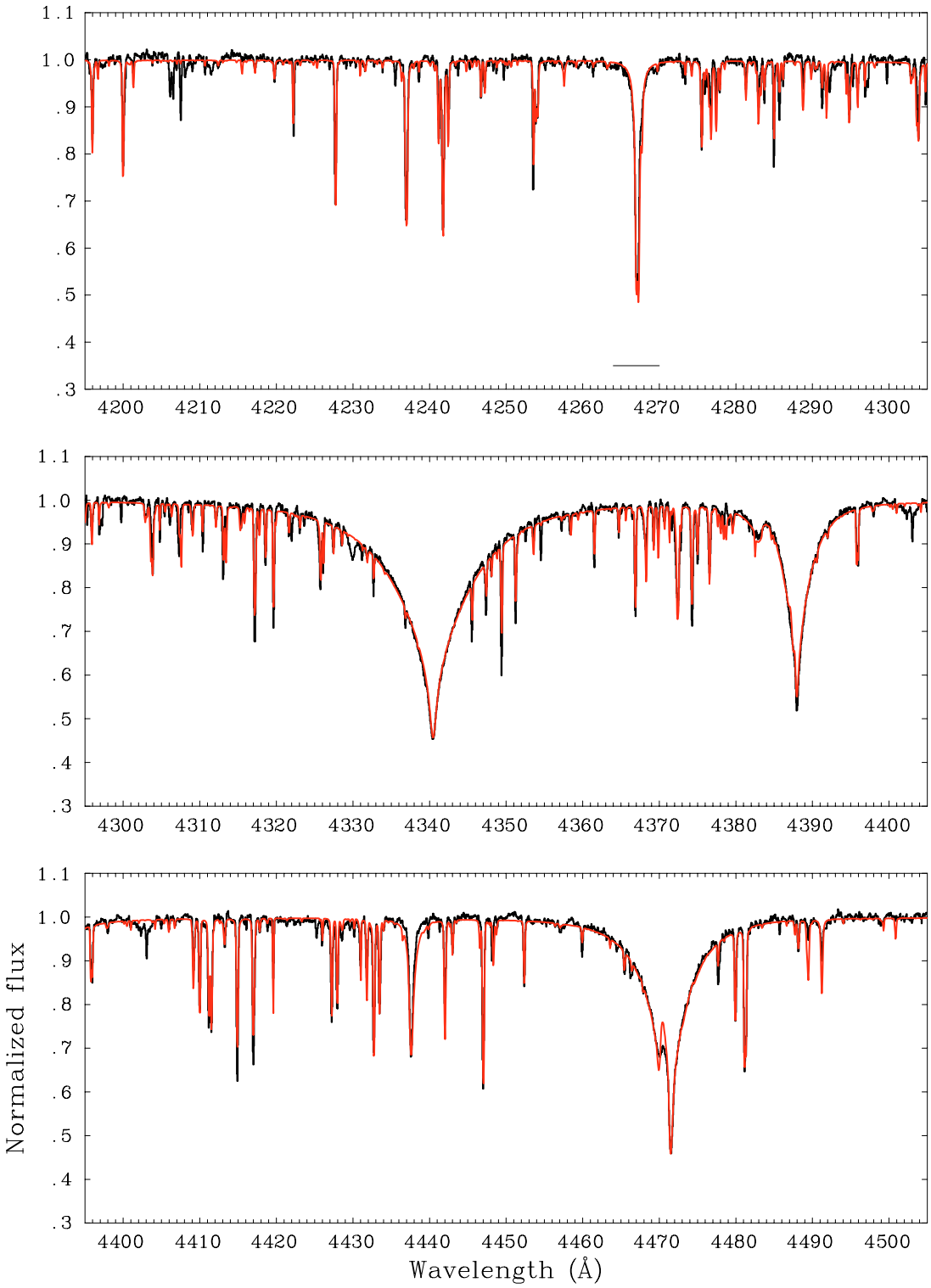

Fig. 6. continued.

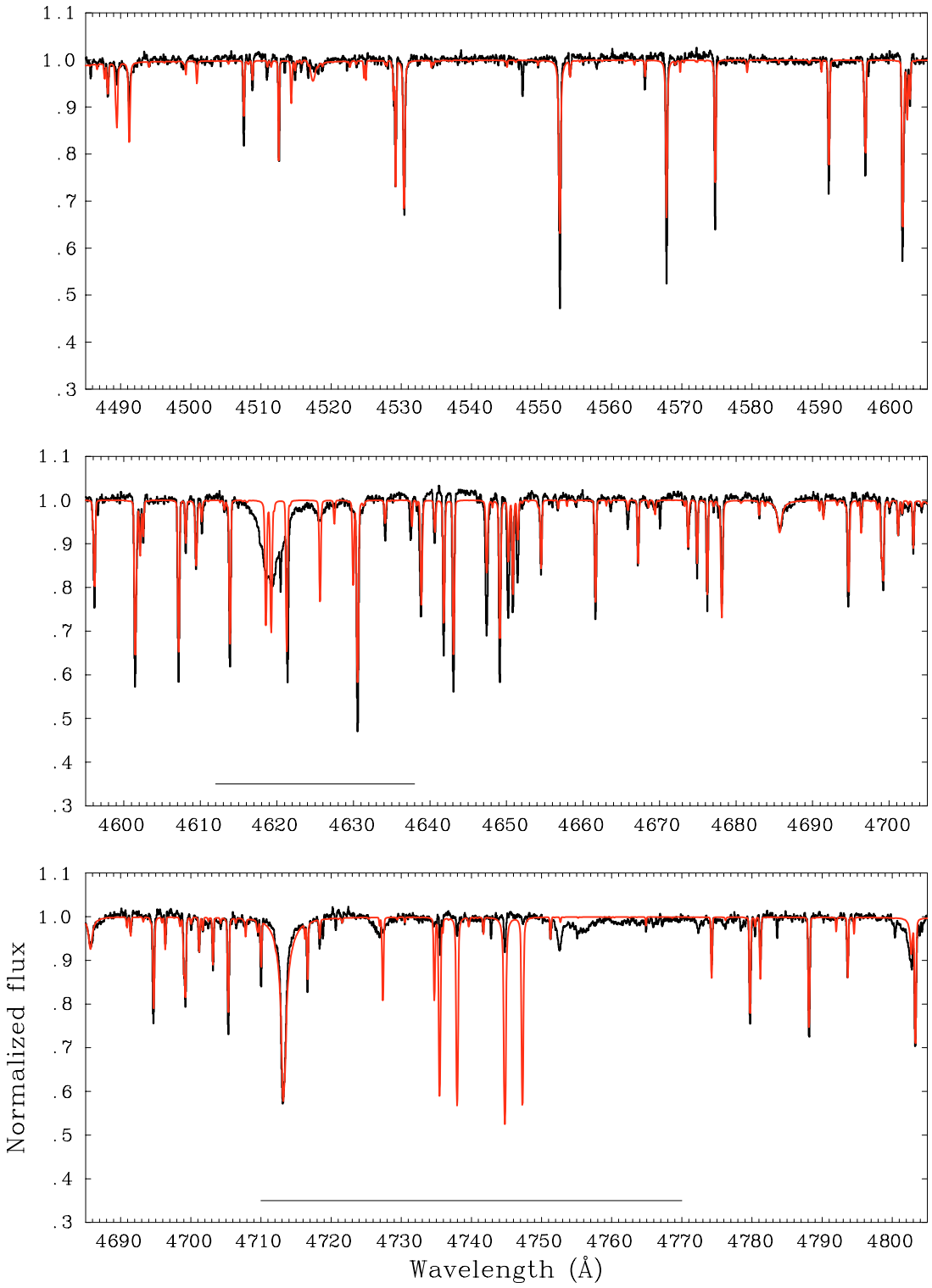

Fig. 6. continued.

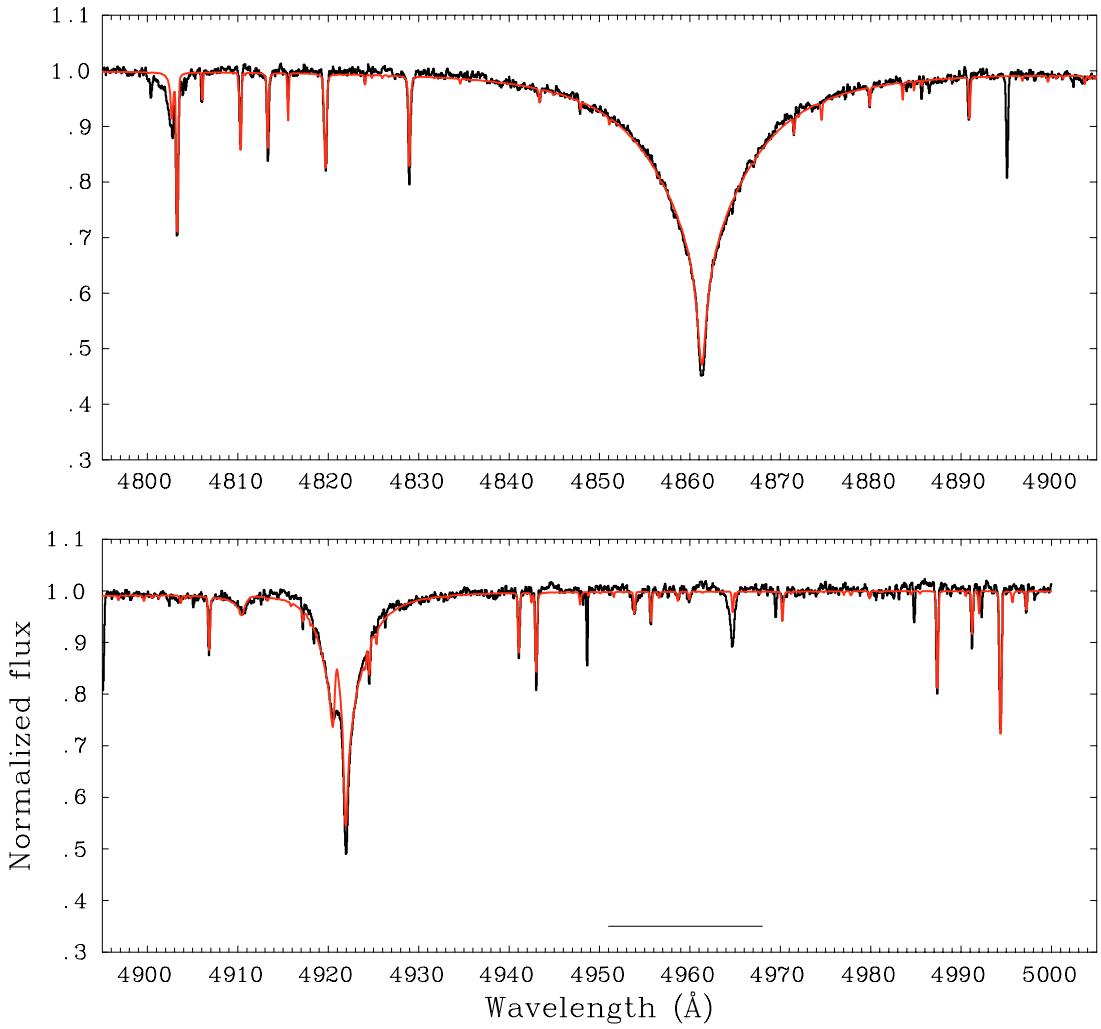

Fig. 6. continued.